ISSN 1674-1056
http://cpb.iphy.ac.cn
http://iopscience.iop.org/cpb
中国物理 B
Chinese Physics
中国物理 Chinese Physics B

Stochastic resonance in an under-damped bistable system driven by harmonic mixing signal

Yan-Fei Jin(靳艳飞)
Citation: Chin. Phys. B . 2018, 27(5): 050501. **doi:** 10.1088/1674-1056/27/5/050501

Journal homepage: http://cpb.iphy.ac.cn; http://iopscience.iop.org/cpb

What follows is a list of articles you may be interested in

Stochastic resonance and synchronization behaviors of excitatory-inhibitory small-world network subjected to electromagnetic induction

Xiao-Han Zhang(张晓函), Shen-Quan Liu(刘深泉)
Chin. Phys. B . 2018, 27(4): 040501. **doi:** 10.1088/1674-1056/27/4/040501

Parameter allocation of parallel array bistable stochastic resonance and its application in communication systems

Jian Liu(刘健), You-Guo Wang(王友国), Qi-Qing Zhai(翟其清), Jin Liu(刘进)
Chin. Phys. B . 2016, 25(10): 100501. **doi:** 10.1088/1674-1056/25/10/100501

Analysis of weak signal detection based on tri-stable system under Levy noise

Li-Fang He(贺利芳), Ying-Ying Cui(崔莹莹), Tian-Qi Zhang(张天骐), Gang Zhang(张刚), Ying Song(宋莹)
Chin. Phys. B . 2016, 25(6): 060501. **doi:** 10.1088/1674-1056/25/6/060501

Achieving high bit rate logical stochastic resonance in a bistable system by adjusting parameters

Yang Ding-Xin, Gu Feng-Shou, Feng Guo-Jin, Yang Yong-Min, Andrew Ball
Chin. Phys. B . 2015, 24(11): 110502. **doi:** 10.1088/1674-1056/24/11/110502

Stochastic resonance in an over-damped linear oscillator

Lin Li-Feng, Tian Yan, Ma Hong
Chin. Phys. B . 2014, 23(8): 080503. **doi:** 10.1088/1674-1056/23/8/080503

Stochastic resonance in an under-damped bistable system driven by harmonic mixing signal*

Yan-Fei Jin(靳艳飞)†

Department of Mechanics, Beijing Institute of Technology, Beijing 100081, *China*

(Received 5 January 2018; revised manuscript received 9 February 2018; published online 26 April 2018)

Stochastic resonance (SR) is studied in an under-damped bistable system driven by the harmonic mixing signal and Gaussian white noise. Using the linear response theory (LRT), the expressions of the spectral amplification at fundamental and higher-order harmonic are obtained. The effects of damping coefficient, noise intensity, signal amplitude, and frequency on spectral amplifications are explored. Meanwhile, the power spectral density (PSD) and signal-to-noise ratio (SNR) are calculated to quantify SR and verify the theoretical results. The SNRs at the first and second harmonics exhibit a minimum first and a maximum later with increasing noise intensity. That is, both of the noise-induced suppression and resonance can be observed by choosing proper system parameters. Especially, when the ratio of the second harmonic amplitude to the fundamental one takes a large value, the SNR at the fundamental harmonic is a monotonic function of noise intensity and the SR phenomenon disappears.

Keywords: stochastic resonance, under-damped bistable system, spectral amplification, harmonic mixing signal

PACS: 05.40.–a, 02.50.–r **DOI:** 10.1088/1674-1056/27/5/050501

1. Introduction

Stochastic resonance (SR) can be considered as a synchronization of noise-induced hopping between the potential wells with a weak periodic forcing.[1–7] For a given nonlinear system, the time-scale matching condition for SR depends on the noise intensity and the period of the driving force. Therefore, noise, nonlinear potential, and periodic driving force have an important effect on the occurrence of SR. For example, Ai and Liu[7] found that an optimal stochastic potential may induce a doubly stochastic resonance (DSR). When the intensity of the stochastic potential is too large, the effect of the double well diminishes and the SR phenomenon disappears. However, most of studies on SR only involve the stochastic systems subjected to one periodic force. Recently, it is found that the harmonic mixing signal plays a constructive role in the context of vibrational resonance or controlling SR.[8–20] Landa and McClintock[8] found the vibrational resonance in an over-damped bistable system subjected to two periodic fields. Gitterman[9] showed that an additional periodic field has control over the shift of the resonance frequency, which is desirable in electronic devices or lasers. Chizhevsky[11,12] reported the experimental evidence of suppression of vibrational higher-order harmonics in a bistable vertical-cavity surface-emitting laser driven by two harmonic signals with very different frequencies. Yang *et al.*[14] investigated the response to the low-frequency of a bistable system perturbed by a low-frequency and a high-frequency excitation. Gammaitoni *et al.*[15,16] proposed the concept of controlling SR by using the periodic mixing signal and developed a general theoretical framework based on a rate equation approach. Schmid *et al.*[17] used the harmonic mixing signal to enhance or suppress the nonlinear SR in an over-damped bistable system. Grigorenko *et al.*[18] investigated the response of a bistable system with a frequency mixing force and reported the SR through the experiment of an iron garnet thin film. Jin *et al.*[19] studied the phenomenon of SR in an asymmetric bistable system subjected to the multiplicative and additive white noises and two periodic fields. Machura *et al.*[20] explored transport properties of the Brownian particles in a symmetric potential driven by the time-periodic biharmonic signals. They demonstrated that the symmetric driving cannot distinguish the direction in the frictionless case. In the case of over-damped motion, the antisymmetric driving leads to zero current. Hence, the study of the SR in nonlinear systems driven by two periodic fields and noise is of great signification.

Generally, most of the dynamical systems using in the study of SR are restricted to over-damped regimes, then the inertial term can be neglected and the theoretical analysis is simplified. However, for intermediate and small damping, the inertial effects should be considered and the under-damped dynamical systems are modeled. The SR phenomenon in the under-damped nonlinear systems and the effects of damping on dynamical behaviors have attracted attention from the scientists of different research fields.[21–31] Du *et al.*[21] and Wu *et al.*[22] found the damping induced stochastic multi-resonance in an under-damped bistable system with delay and without delay, respectively. Saikia[23] showed that the average input energy displays a peaking behavior with the damping coefficient. That is, damping plays a crucial role in the nature of SR in the multistable system. Lindner *et al.*[25] in-

*Project supported by the National Natural Science Foundation of China (Grant No. 11772048).

†Corresponding author. E-mail: jinyf@bit.edu.cn

© 2018 Chinese Physical Society and IOP Publishing Ltd

vestigated the non-equilibrium dynamics of massive damped Brownian particles in an asymmetric periodic potential driven by colored noise. They demonstrated that the finite inertia can enhance the noise-induced transport in a ratchet potential and that for this transport there exhibits an optimal temperature of the embedding bath. Kang *et al.*[26,27] explored the SR phenomenon in an under-damped Duffing oscillator by using the moment method under the weak noise limit. Jin *et al.*[29,30] studied the noise-induced resonances in an under-damped periodic potential driven by colored noise and correlated noise, respectively. Xu *et al.*[31] implemented a numerical investigation of SR in the under-damped bistable system subjected to a weak asymmetric dichotomous noise and a periodic signal. Therefore, an under-damped bistable system is adopted to demonstrate the effects of the harmonic mixing signal on SR in this paper.

The objective of this investigation is to analyze SR phenomenon at fundamental and higher-order harmonic in an under-damped bistable system driven by harmonic mixing signal and Gaussian white noise. Using the LRT, the analytic expressions of the spectral amplification are derived at the fundamental and higher-order harmonic. The effects of the system parameters on the spectral amplification are discussed in Section 2. In Section 3, the system responses, PSD and SNR are calculated to demonstrate the SR and verify the theoretical results. Finally, some conclusions are drawn in Section 4.

2. Spectral amplification

The model of concern is an under-damped particle moving in a bistable potential system, which is driven by Gaussian white noise and a harmonic mixing signal

$$\frac{\mathrm{d}^2x}{\mathrm{d}t^2} = -\gamma\frac{\mathrm{d}x}{\mathrm{d}t} - \frac{\partial U(x)}{\partial x} + G(t) + \sqrt{2\gamma D}\zeta(t), \tag{1}$$

where γ is the damping coefficient, $U(x) = -ax^2/2 + bx^4/4$ denotes a symmetric bistable potential function with a potential barrier $\Delta U = a^2/4b$, D denotes the noise intensity, the noise term $\zeta(t)$ is Gaussian white noise with zero mean and autocorrelation function as follows:

$$\langle\zeta(t)\rangle = 0, \ \ \langle\zeta(t)\zeta(t')\rangle = \delta(t-t'). \tag{2}$$

The harmonic mixing signal $G(t)$ is given by

$$G(t) = A[\sin(\Omega t) + \varepsilon\sin(2\Omega t)], \tag{3}$$

where A is the fundamental amplitude, ε is the ratio of the second harmonic amplitude to A, and Ω is the frequency of signal.

Let $y(t) = \dot{x}(t)$, equation (1) can be rewritten as follows:

$$\begin{cases} \dot{x}(t) = y(t), \\ \dot{y}(t) = -\gamma y(t) + ax(t) - bx^3(t) + \sqrt{2\gamma D}\zeta(t) + G(t). \end{cases} \tag{4}$$

In the absence of any excitation (i.e., $G(t) = 0$, $\zeta(t) = 0$), equation (4) has one unstable equilibrium state $E_0 = (0,0)$ and two stable equilibrium states $E_\pm = (\pm\sqrt{a/b}, 0)$ for $a > 0, b > 0$.

The corresponding Fokker–Planck equation of Eq. (4) is found to be

$$\begin{aligned} \frac{\partial p}{\partial t} &= -\frac{\partial}{\partial x}(yp) - \frac{\partial}{\partial y}\left[(-\gamma y + ax - bx^3 + G(t))p\right] \\ &\quad + \gamma D\frac{\partial^2}{\partial y^2}p, \end{aligned} \tag{5}$$

where $p = p(x,y,t\,|x_0,y_0,t_0)$.

According to Eq. (5), the quasi-stationary probability density is obtained as follows:

$$p_{\mathrm{st}}(x,y) = N\exp\left[-\frac{\tilde{U}(x,y)}{D}\right], \tag{6}$$

where the modified potential function $\tilde{U}(x,y) = y^2/2 - ax^2/2 + bx^4/4 - xG(t)$ and N is the normalization constant.

From Eq. (6), the transition rates out of $E_\pm$ can be obtained under the adiabatic limit condition[1]

$$W_\pm = W_0\exp\left(\pm\frac{1}{D}\sqrt{\frac{a}{b}}G(t)\right), \tag{7}$$

where W_0 stands for Kramers rate of Eq. (1) driven only by noise, and the expression can be given by[26]

$$W_0 = \frac{1}{2\sqrt{2}\pi}\left(\sqrt{\gamma^2+4a} - \gamma\right)\exp\left(-\frac{1}{D}\Delta U\right). \tag{8}$$

Using the two-state theory of SR, $n_\pm$ is defined as the occupation probabilities of the stable states $E_\pm$. Then, the master equation for the occupation probabilities $n_\pm$ is found to be

$$\dot{n}_\pm(t) = -[W_\pm(t) + W_\mp(t)]n_\pm(t) + W_\pm(t). \tag{9}$$

Based on the definition of time-dependent mean value $\langle x(t)\rangle = \sqrt{a/b}[n_+(t) - n_-(t)]$ and Eq. (9), the differential equation for $\langle x(t)\rangle$ can be derived as

$$\frac{\mathrm{d}\langle x(t)\rangle}{\mathrm{d}t} = -[W_+(t) + W_-(t)]\langle x(t)\rangle + [W_+(t) - W_-(t)]. \tag{10}$$

For the weak signal limit, the expansion of Eq. (7) reads

$$W_\pm = W_0\left[1 \pm \frac{1}{D}\sqrt{\frac{a}{b}}G(t) + \frac{a}{2bD^2}G^2(t) \pm \cdots\right]. \tag{11}$$

Substituting Eq. (11) into Eq. (10) leads to the analytical solution in the stationary limit

$$\langle x(t)\rangle = M_0 + \sum_{n=1}^{\infty} 2M_n\cos(n\Omega t + \phi_n), \tag{12}$$

where the amplitudes M_n bring in an additional phase lag ϕ_n for each Fourier component.

Then, the spectral amplification $\eta_i = \left(2M_i/A\sqrt{1+\varepsilon^2}\right)^2$ $(i = 1,2,3)$ at the i-th harmonic are obtained within the LRT[16]

$$\eta_1(\omega = \Omega) = \frac{a}{D^2(1+\varepsilon^2)b}\frac{4W_0^2}{4W_0^2 + \Omega^2}, \tag{13}$$

$$\eta_2(\omega = 2\Omega) = \frac{a\varepsilon^2}{D^2(1+\varepsilon^2)b}\frac{W_0^2}{W_0^2 + \Omega^2}, \tag{14}$$

$$\eta_3(\omega = 3\Omega) = \frac{A^4 W_0^2 a^3}{8D^6(1+\varepsilon^2)b^3} \times \left[(W_0^2+\Omega^2)(4W_0^2+\Omega^2)(4W_0^2+9\Omega^2)\right]^{-1} \times \left[\frac{(W_0^2+\Omega^2)(16W_0^2+9\Omega^2)}{18} - \frac{\varepsilon^2\tilde{A}}{3(4W_0^2+\Omega^2)}\sin\beta + \frac{\varepsilon^4}{2}\left(16W_0^4+\Omega^4-7W_0^2\Omega^2\right)\right], \quad (15)$$

where

$$\tilde{A} = \left[(64W_0^6+\Omega^6-9W_0^2\Omega^4+36W_0^4\Omega^2)^2 + 36W_0^2\Omega^6(\Omega^2-2W_0^2)^2\right]^{1/2},$$

$$\beta = \arctan\left[\left(64W_0^6+\Omega^6-9W_0^2\Omega^4+36W_0^4\Omega^2\right) \Big/ 6W_0\Omega^3\left(\Omega^2-2W_0^2\right)\right].$$

To understand the above theoretical results (13)–(15), one can turn to a case study, where the system parameters are chosen as $a = b = 1$ and $A = 0.01$. Figures 1–3 show the behaviors of the spectral amplification η_i $(i = 1,2,3)$ as a function of D for different γ, ε, and Ω. The curves of η_i $(i = 1,2)$ display a bell shape with the increase in D and SR exists. In Fig. 1, the value of η_i $(i = 1,2,3)$ increases and the position of the peak shifts to the left side with decreasing γ. Especially, the curve of η_3 shows two maximums and one minimum with increasing D in Fig. 1(c). That is, both of noise-induced suppression and resonance are found in the spectral amplification at the third harmonic. While the noise-induced suppression disappears as the damping γ is increased.

In Fig. 2, the value of η_1 decreases with the increase in ε, while the value of η_2 increases with the increase of ε (see Figs. 2(a) and 2(b)). This phenomenon happens because the parameter ε denotes the ratio of the second harmonic amplitude to the fundamental one. Thus, with the increase of ε, the second term in the harmonic mixing signal has a great effect on SR. From Fig. 2(c), the value of the peak increases with increasing ε in the case of $\varepsilon > 1$ and the noise-induced suppression disappears for $\varepsilon = 0.5$. In other words, when the ratio of the second harmonic amplitude to the fundamental one is

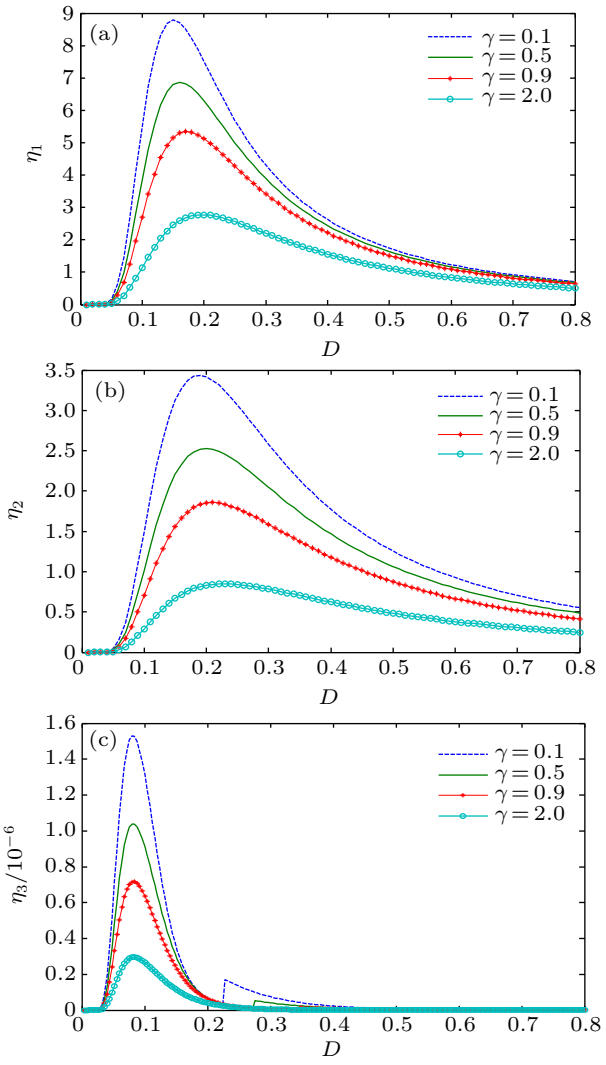


Fig. 1. (color online) Spectral amplification η_i $(i = 1,2,3)$ versus noise intensity D for $\varepsilon = 1$, $\Omega = 0.1$, and different γ.

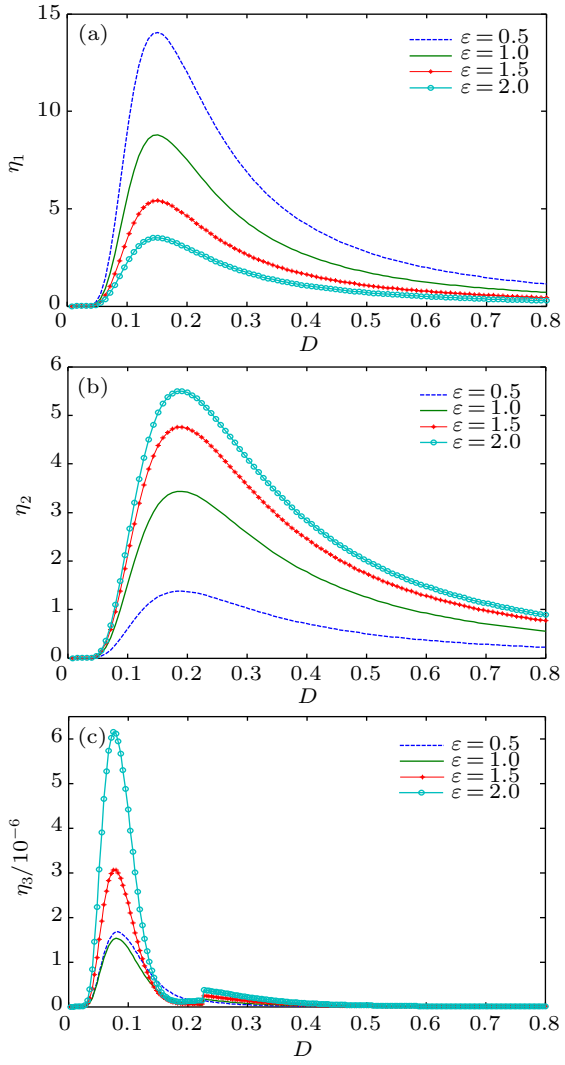


Fig. 2. (color online) Spectral amplification η_i $(i = 1,2,3)$ versus noise intensity D for $\gamma = 0.1$, $\Omega = 0.1$, and different ε.

small, the interaction between the two parts of the harmonic mixing signal is weak. The first part of harmonic mixing signal plays a major role in the occurrence of SR for $\varepsilon < 1$.

In Fig. 3, the values of η_i $(i = 1, 2)$ increase and the positions of the peak shift to the left side with decreasing Ω. It is observed that the optimal noise intensity $D_{\rm op}$ for SR increases with increasing Ω. The bimodal structure is observed in the curve of η_3 for small Ω. When $\Omega = 0.1$, the noise-induced suppression disappears in Fig. 3(c). For the generation of the third harmonic, the effect of resonance and suppression is really small compared with that at first and second harmonics.

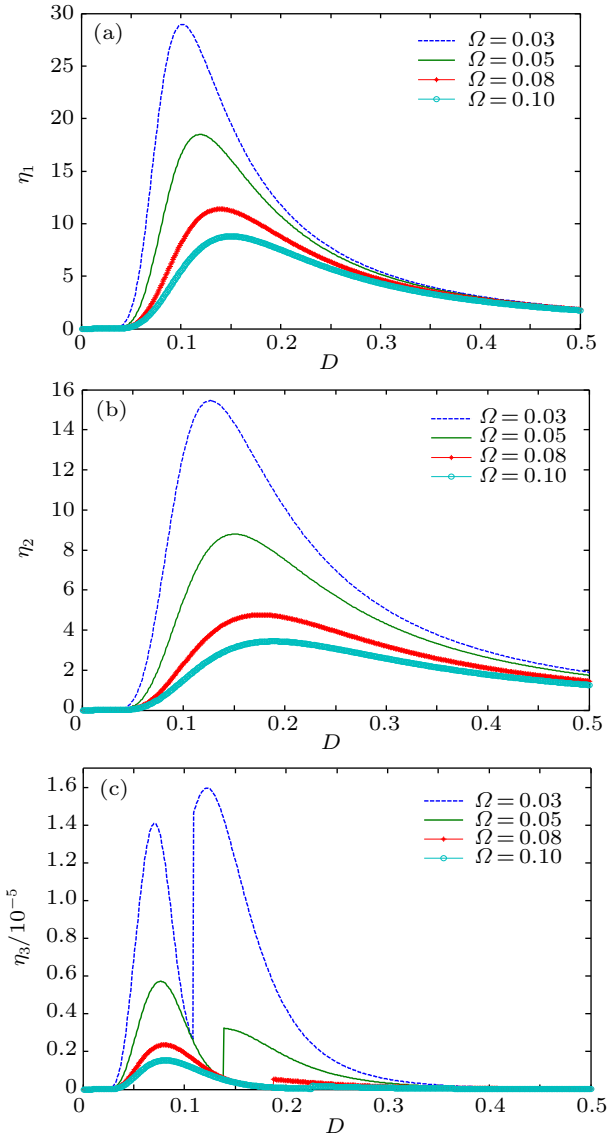


Fig. 3. (color online) Spectral amplification η_i $(i = 1, 2, 3)$ versus noise intensity D for $\gamma = 0.1$, $\varepsilon = 1$, and different Ω.

3. Numerical results

To better understand the influences of harmonic mixing signal on SR and verify the above theoretical results, the numerical results of Eq. (1) are presented by using the fourth-order Runge–Kutta algorithm in this section. In the following analysis, the PSD and SNR are calculated to measure the SR phenomena. It is convenient to quantify SR phenomenon by the intensity of a peak in the PSD and the resonance peak in the SNR.

3.1. Power spectral density

Figure 4 shows the time history and the phase trajectory at four different levels of noise intensity. In Fig. 4(a), the particle stays in the right potential well for weak noise intensity $D = 0.02$. With the increase in noise intensity (i.e., $D = 0.12$ in Fig. 4(c)), the particle switches almost periodically between the right and the left potential well. Namely, the synchronization between noise-induced hopping and the weak signal takes place for a suitable dose of noise intensity. If the noise intensity continues to increase (i.e., $D = 0.3$ in Fig. 4(d)), the noise-induced hopping events between the potential wells will happen more frequently, where the statistical synchronization vanishes and the SR effect is weakened.

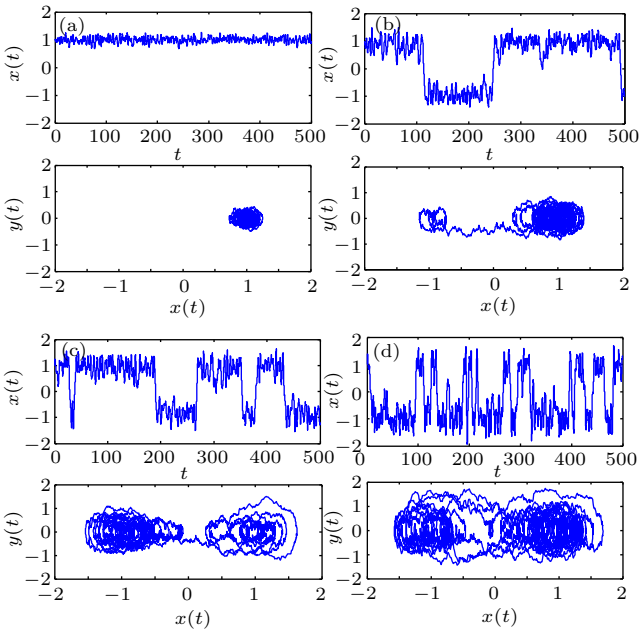


Fig. 4. (color online) Time history and phase trajectory of the system (1) for $a = b = 1$, $\gamma = 0.9$, $A = 0.01$, $\Omega = 0.1$, $\varepsilon = 1$. (a) $D = 0.02$; (b) $D = 0.08$; (c) $D = 0.12$; (c) $D = 0.3$.

The PSD of the mean value $\langle x(t) \rangle$ is plotted to characterize the SR at first and second harmonic in Figs. 5 and 6. From Figs. 5 and 6, there are two peaks appearing at $\omega = \Omega/2\pi$ and $2\omega = \Omega/\pi$, respectively. That is, the SR phenomenon happens at first and second harmonic, which is observed also from the theoretical results (see Figs. 1–3). The intensity of the peak in PSD decreases with increasing γ as shown in Fig. 5. Compared with Fig. 5(a), the positions of peaks in Fig. 6(a) are changed by choosing different Ω. It is seen from Fig. 6 that the intensity of the peak in PSD increases with the increase in A.

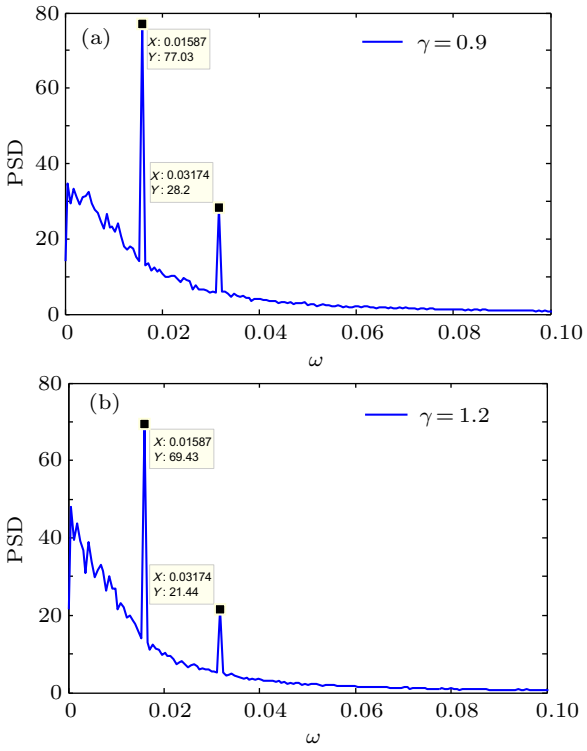


Fig. 5. The PSD of $\langle x(t)\rangle$ for $a = b = 1$, $A = 0.1$, $\Omega = 0.1$, $D = 0.15$, $\varepsilon = 1$. (a) $\gamma = 0.9$; (b) $\gamma = 1.2$.

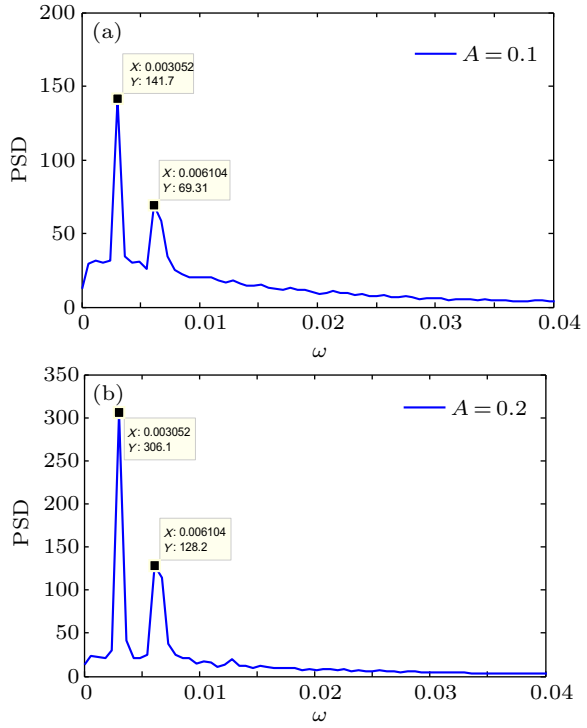


Fig. 6. The PSD of $\langle x(t)\rangle$ for $a = b = 1$, $\gamma = 0.9$, $\Omega = 0.02$, $D = 0.15$, $\varepsilon = 1$. (a) $A = 0.1$; (b) $A = 0.2$.

3.2. Signal-to-noise ratio

In the following analysis, the signal-to-noise ratio (SNR) is introduced as a characteristic measure of SR. The SNR is calculated by $\mathrm{SNR} = 10\log_{10}(S/N)$ dB, where S and N are the amplitudes of the signal and noise background respectively. The S is determined directly from the power spectrum at the driving frequency of the external periodic signal, and N is the average of these amplitudes corresponding to 10 frequency values around the driving frequency in the power spectrum. Here, the SNR at the Ω and 2Ω are defined as SNR_1 and SNR_2, respectively. The influences of noise intensity D, signal amplitude A, driving frequency Ω, and the ratio of the second harmonic amplitude to the fundamental one ε on the SNR_1 and SNR_2 are discussed in Figs. 7–9. It is seen that the curves of SNR_1 vs. D exhibit a minimum first and a maximum later as shown in Fig. 7(a). That is, both of the noise-induced suppression and resonance are found in the curves of SNR_1. From Fig. 7(b), the noise-induced suppression disappears and only the noise-induced resonance appears in the curves of SNR_2 vs. D for the case of $A = 0.2$. It is found that the values of SNR_1 and SNR_2 increase with the increase of A, which coincide with the results shown in Fig. 6.

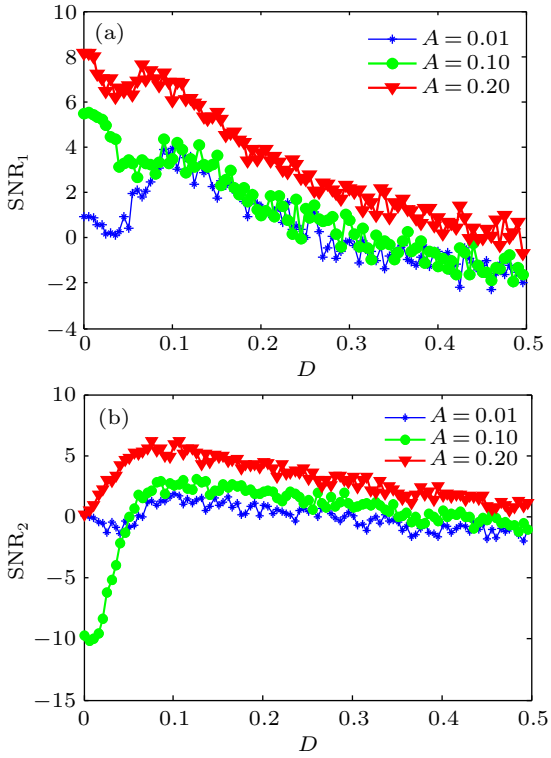


Fig. 7. (color online) The SNR_1 and SNR_2 of the system (1) as a function of noise intensity for $a = b = 1$, $\gamma = 0.9$, $\varepsilon = 1$, $\Omega = 0.1$ with different A.

The effects of Ω on the SNR are shown in Fig. 8. It is found that the curves of SNR_1 and SNR_2 display a minimum first and a maximum later with increasing D. When the values of Ω increase, the peak values of SNR_1 and SNR_2 decrease. Meanwhile, the positions of peak in SNR_1 and SNR_2 moves to right side with the increase of Ω. It is clear that the theoretical results in Fig. 3 agree with the numerical results as shown in Fig. 8.

In Fig. 9, the SNR is a function of D for $A = 0.1$ with different ε. When $\varepsilon = 0.5$ and $\varepsilon = 1.0$, both of the SNR_1 and

SNR_2 manifest the noise-induced suppression and SR at certain values of noise intensity. At the same time, the values of SNR_1 are bigger than those of SNR_2 for $\varepsilon = 0.5$ and $\varepsilon = 1.0$. For $\varepsilon = 3.0$, the curves of the SNR_1 and SNR_2 exhibit the suppression and resonance simultaneously. However, the values of SNR_2 are bigger than those of SNR_1 for this case. This phenomenon can be explained as the amplitude of $\sin(2\Omega t)$ is bigger than that of $\sin(\Omega t)$. When ε continues to increase (i.e., $\varepsilon = 5.0$), both of the noise-induced suppression and resonance in SNR_1 disappear (see Fig. 9(a)). On the other hand, the SNR_2 increases and shows a single-peak structure in Fig. 9(b), which indicates that the second term in the harmonic mixing signal has a dominant effect on SR in this case. That is, SR phenomenon can only be found at 2Ω when ε takes a big value. From Fig. 9, the value of SNR_1 decreases and the value of SNR_2 increases with the increase in ε, which is consistent with the theoretical results shown in Fig. 2.

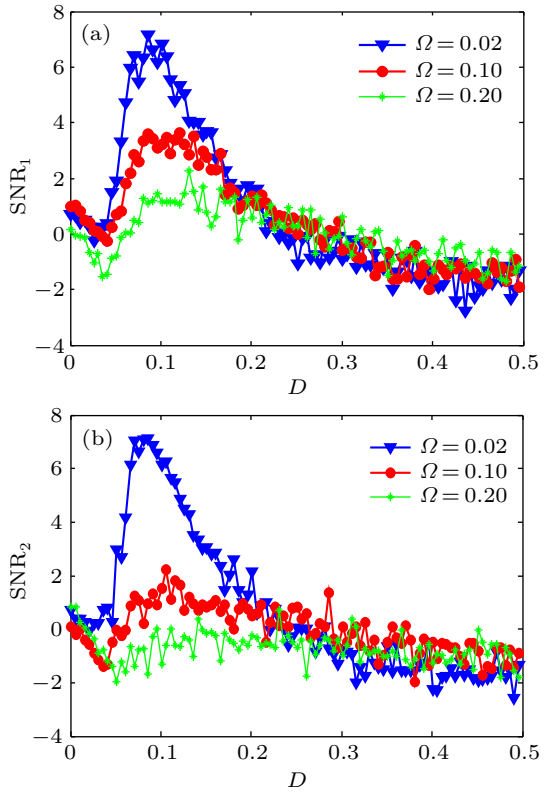


Fig. 8. (color online) The SNR_1 and SNR_2 of system (1) as a function of noise intensity for $a = b = 1$, $\gamma = 0.9$, $\varepsilon = 1$, $A = 0.01$ with different Ω.

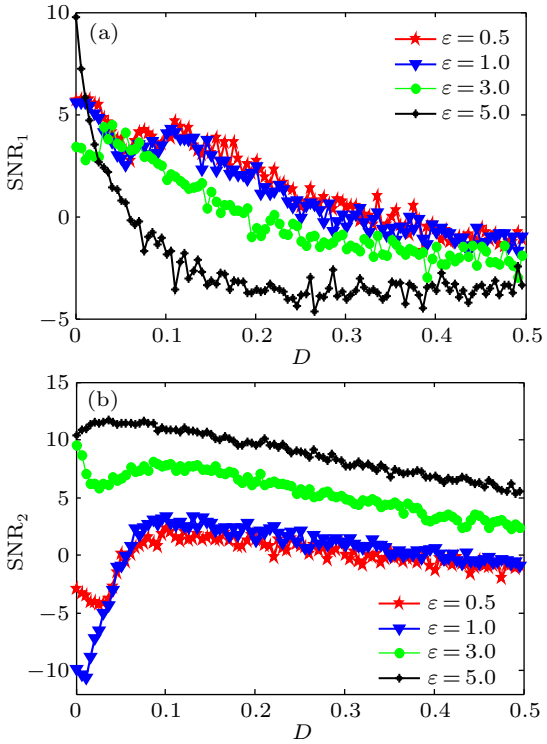


Fig. 9. (color online) The SNR_1 and SNR_2 of the system (1) as a function of noise intensity for $a = b = 1$, $\gamma = 0.9$, $\Omega = 0.1$, $A = 0.1$ with different ε.

4. Conclusion

The phenomenon of SR is analyzed in an under-damped bistable system driven by harmonic mixing signal and Gaussian white noise. The expressions of spectral amplification at fundamental and higher-order harmonic are obtained by using the LRT. It is observed that the curves of the spectral amplification at first and second harmonic show the pronounced single-peak as noise intensity increases. The spectral amplification at third harmonic has a bimodal structure with the increase of noise intensity. That is, the noise-induced suppression and resonance can be found at the third harmonic. This bimodal structure can change to a unimodal one by increasing damping and signal frequency or decreasing the ratio of the second harmonic amplitude to the fundamental one. Moreover, the values of the spectral amplification at third harmonic are very smaller compared with those at first and second harmonic. The PSD and SNRs at the fundamental and second harmonic are calculated numerically to quantify the SR phenomenon and verify the theoretical results. It is shown that the curves of SNR exhibit a minimum first and a maximum later as the noise intensity increases. That is, both of the noise-induced suppression and resonance are found in this system. The values of SNR increase with increasing amplitude and decreasing signal frequency. The SNR at the fundamental harmonic is a monotonic function of noise intensity by choosing a certain value of the ratio of the second harmonic amplitude to the fundamental one.

References

[1] Gammaitoni L, Hänggi P, Jung P and Marchesoni F 1998 *Rev. Mod. Phys.* **70** 223
[2] McNamara B and Wiesenfeld K 1989 *Phys Rev A* **39** 4854
[3] Hu G, Nicolis G and Nicolis C 1990 *Phys. Rev. A* **42** 2030
[4] Xu Y, Wu J, Du L and Yang H 2016 *Chaos Solit. Fract.* **92** 91
[5] Jin Y F, Ma Z M and Xiao S M 2017 *Chaos Solit. Fract.* **103** 470
[6] Xu P F, Jin Y F and Xiao S M 2017 *Chaos* **27** 113109
[7] Ai B Q and Liu L G 2007 *J. Stat. Mech.* **2007** P02019
[8] Landa P S and Mcclintock P V E 2000 *J. Phys. A* **33** L433
[9] Gitterman M 2001 *J. Phys. A* **34** L355

[10] Jung P and Talkner P 1995 *Phys. Rev. E* **51** 2640
[11] Chizhevsky V N 2015 *Phys. Rev. E* **92** 032902
[12] Chizhevsky V N 2014 *Phys. Rev. E* **90** 042924
[13] Yang J H and Liu X B 2010 *Chaos* **20** 033124
[14] Yang J H, Sanjuán M A F and Liu H G 2016 *Commun. Nonlinear Sci. Numer. Simulat.* **30** 362
[15] Gammaitoni L, Löcher M, Bulsara A, Hänggi P, Neff J, Wisesnfeld K, Ditto W and Inchiosa M E 1999 *Phys. Rev. Lett.* **82** 4574
[16] Löcher M, Inchiosa M E, Neff J, Bulsara A, Wiesenfeld K, Gammaitoni L, Hänggi P and Ditto W 2000 *Phys. Rev. E* **62** 317
[17] Schmid G and Hänggi P 2005 *Physica A* **351** 95
[18] Grigorenko A N, Nikitin P I and Roschepkin G V 1996 *J. Appl. Phys.* **79** 6113
[19] Jin Y F, Xu W and Xu M 2005 *Chin. Phys. Lett.* **22** 1061
[20] Machura L, Kostur M and Luczka J 2010 *Chem. Phys.* **375** 445
[21] Du L C and Mei D C 2011 *Physica A* **390** 3262
[22] Wu J and Xu Y 2014 *Discrete Dyn. Nat. Soc.* **2014** 850361
[23] Saikia S 2014 *Physica A* **416** 411
[24] Hennig D, Schimansky-Geier L and Hänggi P 2009 *Phys. Rev. E* **79** 041117
[25] Lindner B, Schimansky-Geier L, Reimann P, Hänggi P and Nagaoka M 1999 *Phys. Rev. E* **59** 1417
[26] Kang Y M, Xu J X and Xie Y 2003 *Acta Phys. Sin.* **52** 802 (in Chinese)
[27] Kang Y M, Xu J X and Xie Y 2003 *Phys. Rev. E* **68** 036123
[28] Xiao S M and Jin Y F 2017 *Nonlinear Dyn.* **90** 2069
[29] Liu K H and Jin Y F 2013 *Physica A* **392** 5283
[30] Jin Y F, Xie W X and Liu K H 2017 *Procedia IUTAM* **22** 267
[31] Xu Y, Wu J, Zhang H Q and Ma S J 2012 *Nonlinear Dyn.* **70** 531